AD-A061 685 COLORADO STATE UNIV FORT COLLINS DEPT OF PHYSICS F/G 20/12
ELECTRONIC PROFILE OF N-INAS ON SEMI-INSULATING GAAS.(U)
OCT 78 H A WASHBURN, J R SITES, H H WIEDER N00014-76-C-0976
UNCLASSIFIED SF15 NL

1 OF
AD
A061685

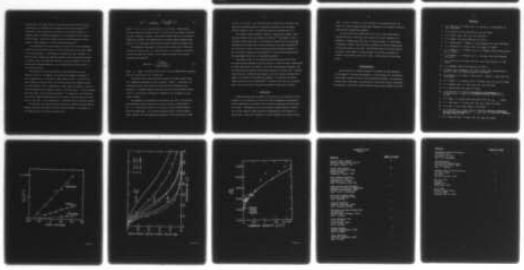

END
DATE
FILMED
2 -- 79
DDC

ELECTRONIC PROFILE OF n-InAs ON SEMI-INSULATING GaAs

H. A. WASHBURN
J. R. SITES
H. H. WIEDER

COLORADO STATE UNIVERSITY

REPORT SF15

(6)

ELECTRONIC PROFILE OF n-InAs ON SEMI-INSULATING GaAs.

(9) Technical Report, October 20, 1978

ONR Contract N00014-76-C-0976

(15)

Contract Authority NR 243-015

(11) 20 Oct 78

(12) 31 p.

by

(10) H. A. Washburn,
J. R. Sites
H. H. Wieder

(14)

Report SF15

Department of Physics
Colorado State University
Fort Collins, Colorado 80523

1473

401 269

78 11 24 014

LB

Unclassified

SECURITY CLASSIFICATION OF THIS PAGE (When Data Entered)

REPORT DOCUMENTATION PAGE

READ INSTRUCTIONS BEFORE COMPLETING FORM

1. REPORT NUMBER: SF15	2. GOVT ACCESSION NO.
3. RECIPIENT'S CATALOG NUMBER	
4. TITLE (and Subtitle): Electronic Profile of n-InAs on Semi-insulating GaAs	5. TYPE OF REPORT & PERIOD COVERED: Technical
6. PERFORMING ORG. REPORT NUMBER	
7. AUTHOR(s): H. A. Washburn, J. R. Sites, and H. H. Wieder	8. CONTRACT OR GRANT NUMBER(s): N00014-76-C-0976
9. PERFORMING ORGANIZATION NAME AND ADDRESS: Colorado State University, Fort Collins, CO, 80523	10. PROGRAM ELEMENT, PROJECT, TASK AREA & WORK UNIT NUMBERS: PE 61153 N, RR 021-02-03, NR 243-015
11. CONTROLLING OFFICE NAME AND ADDRESS: Office of Naval Research, Electronic and Solid State Science Program, Arlington, VA, 22217	12. REPORT DATE: October 20, 1976
	13. NUMBER OF PAGES: 26
14. MONITORING AGENCY NAME & ADDRESS (if different from Controlling Office)	15. SECURITY CLASS. (of this report): Unclassified
	15a. DECLASSIFICATION/DOWNGRADING SCHEDULE

16. DISTRIBUTION STATEMENT (of this Report)

Approved for public release; distribution unlimited.

17. DISTRIBUTION STATEMENT (of the abstract entered in Block 20, if different from Report)

18. SUPPLEMENTARY NOTES

ONR Scientific Officer
Telephone: (202) 696-4218

19. KEY WORDS (Continue on reverse side if necessary and identify by block number)

Indium arsenide	Heteroepitaxy
Surface quantization	Shubnikov-de Haas
Surface mobility	Ion beam texturing
Effective mass	MIS structures

20. ABSTRACT (Continue on reverse side if necessary and identify by block number)

Electron density and mobility are measured in three regions of InAs epilayers on GaAs substrate: (1) The interfacial layer shows an increase in density and decrease in mobility over a 3 μm* distance; (2) the bulk of the epilayer has $n \sim 10^{16}\text{cm}^{-3}$, $\mu \sim 10^{5}\text{cm}^{2}/\text{V-sec}$; (3) the front surface, accumulated at zero bias, displays surface quantization effects and an enhanced effective mass.

*micron

DD FORM 1 JAN 73 1473 EDITION OF 1 NOV 65 IS OBSOLETE S/N 0102-014-6601

Unclassified

SECURITY CLASSIFICATION OF THIS PAGE (When Data Entered)

approx. 1/10 to the 16th power cc, mu approx. 10000 sq. cm/V-sec

ELECTRONIC PROFILE OF n-InAs ON SEMI-INSULATING GaAs

H. A. Washburn,* J. R. Sites, and H. H. Wieder†

Department of Physics

Colorado State University

Fort Collins, Colorado, 80523

ABSTRACT

The electron density and mobility of VPE grown 15 μm n-type indium arsenide epilayers have been determined as a function of distance from the gallium arsenide substrate. Both epilayer surfaces show significant increases in density and decreases in mobility from the bulk values (10^{15}-10^{16}cm^{-3} and 10^{5}cm^{2}/V-sec at 77°K). The interfacial, or back, surface is apparently dominated by defects to a depth of about 3 μm. The density and mobility profiles are roughly exponential; integrated values are 1.6×10^{13}cm^{-2} and 2×10^{3}cm^{2}/V-sec. The front surface, highly dependent on applied gate bias, has a density range in accumulation from 0 to 5×10^{12}cm^{-2} and mobility from 2.5×10^{4} to 3×10^{3}cm^{2}/V-sec. The parameters for both surfaces are essentially temperature independent below 80°K. The front surface effective mass increases with electron density from its band edge value of 0.0215 m_e to nearly 0.06 m_e.

---

*Present address: Intel Magnetics, Santa Clara, CA, 95051

†Permanent address: Electronic Materials Sciences Div., NOSC, San Diego, CA, 92152

I. INTRODUCTION

Many semiconductor applications utilize a conductive epitaxial layer deposited on a high resistance substrate. In general the electronic depth profile of such an epilayer is not homogeneous, and it may be misleading to characterize the layer with average electronic parameters such as carrier density, mobility, and effective mass. Furthermore, when one has hetero-epitaxy, different materials for the substrate and epilayers, there are additional complications due to inhomogeneities in composition and defect density at the interface. Finally, when the epitaxial layer consists of a high mobility, low effective mass material, it may well be necessary to evaluate the effects of quantization of the surface carriers.

The purpose of this paper is to evaluate the inhomogeneities normal to the surface of high mobility n-type indium arsenide layers grown on semi-insulating gallium arsenide substrates. Through a variety of measurements, primarily electrical and galvanomagnetic, we have been able to obtain (1) a profile of the electron density and mobility at the epilayer-substrate interface, (2) the bulk-like properties of the main portion of the epilayer, and (3) the density, mobility, effective mass, and quantization effects of electrons in the surface accumulation layer.

II. SAMPLE PREPARATION

InAs epilayers were deposited on <100>-oriented semi-insulating GaAs substrates by means of an open-tube chemical vapor phase disproportionation process.[1-3] Gaseous AsH_3, HCℓ and H_2 were transported at essentially constant (slightly larger than atmospheric) pressure along a quartz reaction chamber placed within a three zone temperature controlled furnace. Inside the chamber, the indium source material, present in the high temperature

zone, reacts with HCℓ. The gaseous reaction products are transported through the second intermediate temperature zone to the low temperature zone where they disproportionate and are deposited in the form of a single crystal InAs layer upon the GaAs substrates.

The lattice constant mismatch and the difference in the thermal expansion coefficients of InAs and GaAs prevent the outright deposition and growth of high quality epilayers. For this reason, a compositionally graded ternary $In_xGa_{1-x}As$ intermediate layer is grown upon the substrate with the grading adjusted to provide an appropriate match to GaAs at one face and to InAs at the other. This compositional grading can relieve much of the strain associated with the interfacial mismatch. InAs epilayers of thickness $d > 10$ μm grown in this manner have a relatively low defect density, a low residual impurity density, and a bulk mobility which approaches theoretically calculated values, based on scattering from ionized impurities and longitudinal optical phonons. Since the compositionally graded region perturbs electrical and galvanomagnetic measurements, it is desirable to keep the thickness of the compositionally graded region as small as practical without sacrificing the crystalline perfection. Fortunately this can be done by means of relatively simple empirical procedures which require an appropriate choice of the temperature of each reactor zone, the temperature gradients between them, the partial pressures of the constituents and the gas flow rates. In this manner the thickness of the interfacial region can be kept to the order of or less than 1 μm.

The samples described below were grown to thicknesses in the range between 10 and 15 μm. The metal-insulator-semiconductor (MIS) structures shown in Figs. 1a and 1b were made by photolithographic procedures; undesired portions of the InAs epilayers were removed by etching while retaining the

portions protected by photoresist. An SiO_2 insulating layer ($\sim$ 0.15 μm thick), was deposited by the low temperature pyrolisis of silane on the clean InAs surfaces. Finally, Ni gate electrodes (shaded area of Fig. 1a and b, typically 3 to 10 mm^2) were deposited and leads attached to the electrodes.

The cross-sections of the complete devices are shown in Fig. 1c which also shows schematically three regions of the epilayer: Surface 1 is a region characterized by electron accumulation; the bulk region is characterized by properties very similar to those of bulk single crystal n-type InAs; surface 2 is the interfacial region adjacent to the semi-insulating GaAs substrate.

III. MEASUREMENT

For most of the electronic measurements described in this paper the indium arsenide MIS structures were mounted in the variable temperature bore of a superconducting magnet. The sample temperature could be varied from 1.6 to 400°K and the transverse magnetic field from 0 to 6 tesla. The apparatus used for dc conductivity and Hall measurements is shown schematically in Figure 2a. For clarity only two switch positions are shown, the other two switch positions are used for permutations of contacts. The currents used were 0.1 or 1.0 ma; these currents do not produce any significant Joule heating of the sample. For some measurements, particularly those involving the thickness dependence of the electrical and galvanomagnetic properties of the epilayers, the gate contact was omitted.

The ac, or differential, mode used in several measurements has the same basic circuit with a small ac voltage added to the gate bias V. In this case, as shown in Fig. 2b, the digital voltmeter is replaced by a

lock-in amplifier referenced to the ac component of the gate bias. Capacitance measurements were made using a bias voltage and a 1 MHz Boonton capacitance meter between the gate and the InAs contacts.

IV. RESULTS

A. Interfacial Region

One of the experimental procedures used was to determine the conductivity and the Hall coefficient of a layer as it was successively thinned by low energy (500 eV) argon ion beam sputtering from 15 microns to zero. The results thus obtained are in general agreement with those from epilayers having a variety of thicknesses.[4] The thickness reduction technique appears to be quite reliable. Using a scanning electron microscope, it is quite obvious (Fig. 3) when the indium arsenide (texture on right side) is etched through to the gallium arsenide (left hand texture). The initial layer and the sputtering process were found to be sufficiently uniform that the entire area is etched through between two examinations separated by 1/2 μm. Furthermore, the vertical dimension of the InAs surface texturing is seen to be less than this value.

The measured values of conductivity σ_o and Hall coefficient R_o are shown in Figure 4 as a function of remaining InAs thickness. The measurements were made at 77 K in low magnetic fields. These results may be interpreted analytically by expressing the electron concentration n(z) and mobility $\mu(z)$ as continuous functions of the direction z normal to the interface. The effective, or measured, value of conducticity is

$$\sigma_o = \frac{e}{d} \int_o^d n(z)\mu(z)dz \ , \qquad (1)$$

and the Hall coefficient in the weak magnetic field approximation is

$$R_o = \frac{e}{\sigma_o^2 d} \int_o^d n(z)\mu^2(z)dz \ , \tag{2}$$

where d is the thickness of the layer.

One can now take differences between measured values of σ_o and R_o to determine n and μ as a function of distance from the substrate:

$$n(z)\mu(z) = \frac{1}{e}\frac{\Delta(\sigma_o d)}{\Delta d} \tag{3}$$

$$n(z)\mu^2(z) = \frac{1}{e}\frac{\Delta(R_o\sigma_o^2 d)}{\Delta d} \ , \tag{4}$$

The values of n and μ extracted in this manner are shown in Figure 5. Note that this procedure basically consists of measuring the electronic properties of the portion of the epilayer removed by each successive milling step. These are independent of the front surface parameters, assuming the front surface is identical following each milling increment.

The behavior of carrier concentration and mobility in Figure 5 is consistent with the model of Baliga and Ghandi[5] in which the defect formation at the interface leads to a carrier density which decreases exponentially as one moves away from the interface. The corresponding mobility is likely to be dominated by defect scattering and to first order is inversely proportional to n. The characteristic distance for our InAs samples is seen from Figure 5 to be about one μm, and at 5 μm and above, the layer is essentially bulk-like. The bulk values for this epilayer shown are somewhat inferior ($\mu = 3.5 \times 10^4 cm^2/V\text{-}sec$; $n = 9 \times 10^{15} cm^{-3}$) to those of other samples investigated.

The metallurgical profile of the GaAs/InAs interface, as revealed by Auger measurements on the sample used for the thickness dependence study, is

also shown in Figure 5. The much sharper transition from gallium to indium dominance (less than 1000 Å) is consistent with what one would expect from vapor phase growth and the abrupt change in texture mentioned above.

B. Front Surface Region

The surface of InAs is known to pin the Fermi level approximately 50 meV above the conduction band minimum.[6] Thus, n-type material has a heavily accumulated surface under zero bias. Schwartz, et al.[7] showed that at 77°K, a high negative bias would bring the surface into deep depletion, and they calculated a surface state density of $2.8 \times 10^{11} cm^{-2}$ and a fixed oxide charge of $+1.5 \times 10^{12} cm^{-2}$. Further measurements made by Wilmsen, et al. are in qualitative agreement.[8]

We have measured the gate voltage dependence of the conductivity and Hall coefficient of MIS InAs structures. The samples used were from a different growth run than those that were milled away in Section IV.A. They had an average electron concentration of $1.3 \times 10^{15} cm^{-3}$ and mobility of $1.4 \times 10^{5} cm/V\text{-}sec$ at 77°K prior to the fabrication of the MIS structure.

The values of the total surface electron density $\langle N_s \rangle$ and average surface mobility $\langle \mu_s \rangle$, combining the effects of the two surfaces, are extracted from the 77°K galvanomagnetic measurements and are shown in Fig. 6a. The analysis procedure, which has been described previously,[9,10] is to divide the epilayer arbitrarily into a bulk-like and a surface-like region. The flat parts of the Fig. 6a curves at large negative bias are interpreted as the depletion region where the front surface carrier transport is the same as that in the bulk, and the values of $\langle N_s \rangle$ and $\langle \mu_s \rangle$ are to be associated with Surface 2, or the interfacial region. This interpretation is supported by the capacitance data shown in Fig. 6b where flat band is seen to coincide

with the kinks in Fig. 6a. The value of the surface electron density when the front surface is in depletion is found to be $1.6 \times 10^{13} cm^{-2}$ and agrees well with the integration of the interfacial density n(z) taken from the sample shown in Fig. 5a. The surface mobility with the front surface at flatband is 2400 cm^2/V-sec and is consistent with the average value of 5b, as weighted by the carrier density.

When the gate voltage is varied so that the front surface becomes accumulated, the total surface density increases. This increase, interpreted as the front surface density, N_{s1}, is shown in Fig. 6c. Extraction of the front surface mobility is somewhat more involved,[10] but leads with semi-quantitative reliability to the values of μ_{s1} also shown in Fig. 6c. The surface mobility becomes quite large as the sample approaches flat band, achieving perhaps the bulk values but in any case larger than that reported in inversion layers.[11] For stronger accumulation, the surface mobility falls monotonically. The dashed curve, shown for comparison, is based on a simple calculation based on diffuse surface scattering using a square well surface potential.[12] It is not clear whether the difference in magnitude is due to a form of screening, to a certain amount of specular reflection, or to the magnitude of the surface potential used.

The following qualitative interpretation is proposed for the average surface mobility of 6a. In depletion, it is simply that of the interfacial layer. As the front surface begins to be accumulated, however, its higher mobility electrons are added to the average electron density in increasing numbers, and the average surface mobility goes up. In strong accumulation, though, the front surface mobility has decreased substantially, probably due to surface scattering, and thus the average surface mobility goes back down.

The values of surface potential shown in Fig. 6d are tenuous at best. Since the Fermi level is strongly pinned in InAs, it is difficult to extract the surface potential from either the quasistatic or high frequency C-V curve. Our simplified approach, therefore, was to take the front surface density from Fig. 6c, estimate the density of states and the shape of the well, and calculate how deep the well must be to accommodate all the states. Each step involves a potential error, but the nearly linear dependence of the result is considered correct.

The procedures described above to obtain the 77°K data were also followed for several other temperatures, and the results allowed extraction of the temperature dependence of the surface parameters. Figure 7a shows the electron density values for the front surface in strong accumulation (V_G = 35 volts), for the bulk of the epilayer and for the back surface. Figure 7b shows the corresponding mobility values. Again, the analysis described in Ref. 10 was used. To first order all three density curves are constant with temperature. If the front surface density for other gate voltages were plotted, then the N_{s1} curve would simply be decreased to lower magnitudes. In all cases, however, it is substantially lower than the back surface density. In the case of the mobilities also, both surface values are nearly constant. The effect of lower gate voltages here is to raise the front surface curve in magnitude. This temperature independence of the surface mobilities contrasts sharply with that of the bulk mobility, which exhibits a strong temperature dependence, attributed to ionized impurity scattering in this temperature range.[9]

C. Surface Quantization

At low temperatures, electrons in the accumulated front surface of an InAs epilayer are found in discrete subbands of the conduction band. Ex-

perimentally, this effect leads to Shubnikov-de Haas oscillations in the conductivity as a function of the magnetic field or gate voltage.[13,14] The period of the oscillations is related to the electron density of a subband, and the temperature dependence of the amplitude to the electron effective mass. One can also deduce electron scattering times from the magnetic field dependence of the oscillation amplitudes.[15]

The Shubnikov-de Haas oscillations can be seen in the dc measurements using the circuit shown in Fig. 2a, but the amplitudes are not large enough for accurate analysis. A differential technique was used, therefore, in which the gate voltage was modulated slightly, and the resulting modulation in voltage across the sample detected with a lock-in amplifier. Two InAs samples were studied extensively, one of them being the same as used in the previous section.

The output of the lock-in amplifier yields curves such as those depicted in Fig. 8. In general, the ground state subband is dominant at gate voltages near flat band and at high magnetic fields. It leads to the peaks labeled 0, while the first and second excited state subbands produce the peaks labeled 1 and 2, respectively. Often there is a mixing of oscillations from more than one subband as shown in the same figure. At gate voltages below flat band, the oscillations disappear. For comparison, the capacitance curve also is shown, demonstrating that the onset of oscillations does indeed occur at flat band. As the temperature is increased these oscillations vanish.

For analysis, the conductivity oscillations are generally plotted against magnetic field and the period in inverse field calculated. The density of the subband $N_{s1}(i)$ can now be extracted from

$$N_{sl}^{(i)} = \frac{e}{\pi\hbar\,\Delta(1/B)} = \frac{4.84 \times 10^{10}}{\Delta(1/B)}\ cm^{-2}, \qquad (5)$$

where i is 0, 1, or 2, and the field B is in tesla. These surface electron densities are shown in Fig. 9, and they show an increase in density with gate voltage as expected. Each higher subband appears at successively higher gate voltages and suggests that still higher energy subbands might appear, if the experiment were pursued to higher voltages and deeper wells.

The temperature dependence of ground state oscillations at three gate voltages are shown in Fig. 10. From this data, it is possible to calculate the effective mass for carriers in the surface potential well using the theoretical dependence[16]

$$\text{Amplitude} \sim \frac{2\pi^2 kT/\hbar\omega_c}{\sinh(2\pi^2 kT/\hbar\omega_c)}, \qquad (6)$$

where $\omega_c = eB/m^*$. The solid curves in Fig. 10, for example were calculated from Eq. 6 with $m^*/me = .02$, .04 and .06.

In practice, some corrections must be made to the data because there is a temperature dependence of the scattering times[17] and because the accumulation layer is in electrical contact with the remainder of the epilayers. We assume, however, that since the front surface mobility shown in Fig. 7 is essentially temperature independent, the lifetimes are very nearly constant.

The weighting of the quantum oscillations by the rest of the epilayer was determined using the analysis of the last section, as elaborated in Ref. 10. The effect is found to be a function of gate voltage, magnetic field and temperature. For a given oscillation peak at constant magnetic field, however, only the temperature dependence of the bulk mobility shown

in Fig. 7 is a factor. For the ground state oscillation at six tesla, the bulk layer shunting resulted in a maximum correction to the calculated effective masses of 20%. The resulting values are plotted in Fig. 11.

The effective masses exhibit a monotonic increase with density, somewhat more dramatic than that observed in silicon.[18] Such behavior can be explained with the Kane model for non-parabolic bands,[19] and the resulting alteration of the dispersion relation produced by the surface potential.[20] The solid curve in Fig. 11 was calculated from the dispersion relation in Ref. 20 using an exponential approximation[21] to the surface potential well. The experimental values are in reasonable agreement.

Also shown in Fig. 11 are effective masses calculated for the first and second excited subbands using data taken at 2.0 and 0.5 tesla, respectively. At these lower fields, the effect of the bulk layer shunting is greater, and the corrections can increase the effective masses by as much as 50%. Although these values are considered less reliable, they also exhibit increases with density of carriers in the respective subbands. The increase of excited subband effective mass is predicted[20] to be greater than that for the ground state, but we do not have sufficient sensitivity to make such a contrast.

V. CONCLUSIONS

Careful attention must be given to the effects of both surfaces of InAs epilayers in the evaluation of electrical and galvanomagnetic measurements. Electron mobilities can easily be over an order of magnitude less than those in the bulk. Furthermore, since the interfacial region between an epilayer and its GaAs substrate shows electronic inhomogeneities that extend for a few microns, it may not be possible to utilize extremely thin layers of this

type. In fact, if there is a lattice mismatch in epitaxial growth, the result is a defect dominated layer whose thickness is a function of the mismatch and the compositional grading.

The zero bias front surface mobility of InAs is also substantially reduced from that of the bulk, and it seems to be quite temperature independent at temperatures below that of liquid nitrogen. It does change considerably, however, when the surface potential is varied, extrapolating to near bulk values at flat band. The effective mass of the front surface electrons is also subject to large changes as the surface potential is varied; it may increase as much as a factor of three above its band edge value.

ACKNOWLEDGEMENTS

We are grateful to Charles Parkerson for growing the InAs epilayers, to John Wager for the Auger measurements, to Curtis Haynes for the SEM work, and to Robert Leisure for use of the superconducting magnet. We appreciate several useful discussions with David Ferry, and we particularly acknowledge the support of the Office of Naval Research under Contract N00014-76-C-0976.

REFERENCES

1. G. R. Cronin, R. W. Conrad, and S. R. Borrello, J. Electrochem. Soc. 113, 1336 (1966).

2. J. P. McCarthy, Solid State Electron. 10, 649 (1967).

3. H. H. Wieder, Appl. Phys. Lett. 25, 206 (1974).

4. H. H. Wieder, Thin Solid Films 41, 185 (1977).

5. B. J. Baliga and S. K. Ghandi, J. Electrochemical Soc. 121, 1646 (1974).

6. C. A. Mead and W. G. Spitzer, Phys. Rev. 134A, 713 (1964).

7. R. J. Schwartz, R. C. Dockerty, and H. W. Thompson, Solid State Electron. 14, 115 (1971).

8. C. W. Wilmsen, L. G. Meiners, and D. A. Collins, Thin Solid Films 46, 331 (1977).

9. J. R. Sites and H. H. Wieder, CRC Crit. Rev. Solid State Sci. 5, 385 (1975).

10. H. A. Washburn, Thin Solid Films 45, 135 (1977).

11. S. Kawagi and Y. Kawaguchi, Proc. Intern. Conf. Phys. Semiconductors, Kyoto; J. Phys. Soc. Japan 21 (Suppl.), 336 (1966).

12. Y. Goldstein, N. B. Grover, A. Many and R. F. Greene, J. Appl. Phys. 32, 2540 (1961).

13. R. J. Wagner, T. A. Kennedy, and H. H. Wieder, Surf. Sci. 73, 545 (1978).

14. H. A. Washburn and J. R. Sites, Surf. Sci. 73, 537 (1978).

15. R. J. Sladek, Phys. Rev. 110, 817 (1958).

16. L. M. Roth and P. N. Argyres, Semiconductors and Semimetals, R. K. Willardson and A. C. Beer, Eds. (Academic, New York, 1977), Vol. 1, p. 159.

17. F. F. Fang, A. B. Fowler and A. Hartstein, Surf. Sci. 73, (1978).

18. J. L. Smith and P. J. Stiles, Phys. Rev. Letters 29, 102 (1972).

19. E. O. Kane, J. Phys. Chem. Solids 1, 249 (1957).

20. G. A. Antcliffe, R. T. Bate, and R. A. Reynolds, Physics of Semimetals and Narrow Gap Semiconductors, D. L. Carter and R. T. Bate, Eds. (Pergamon, New York, 1971), p. 487.

21. M. E. Alfereiff and C. B. Duke, Phys. Rev. 168, 832 (1968).

FIGURE CAPTIONS

Figure 1. (a) Sample configuration refered to as the cloverleaf.
(b) Bridge shaped sample configuration.
(c) Cross section of InAs MOS structure.

Figure 2. Schematic of the circuitry used for resistivity and Hall coefficient measurements (a) dc (b) differential.

Figure 3. SEM photograph showing contrast in texture between indium arsenide (right) and gallium arsenide (left) when both are exposed to 500 eV ion milling. Region shown is 60 by 80 μm.

Figure 4. Measured values of conductivity (a) and Hall coefficient (b) as a function of thickness of the etched InAs. Sample A.

Figure 5. Profile of carrier density (a), mobility (b), and metallurgical composition (c) in the vicinity of the GaAs/InAs interface. Sample A.

Figure 6. Gate voltage dependence of (a) total surface electron density and effective mobility. (b) Capacitance at 1 MHz. (c) Front surface electron density and mobility. Dashed line is calculated mobility. (d) Front surface potential. Sample B.

Figure 7. Temperature dependence of (a) electron density, (b) mobility, of each of the three InAs regions. Sample B.

Figure 8. Shubnikov-de Haas oscillations as a function of gate voltage for four magnetic fields. Oscillations are associated with the ground state (0), first (1), and second (2) excited subbands. Also shown for the flat band reference is the 4°K capacitance curve. Sample B.

Figure 9. Subband densities as a function of gate voltage.

Figure 10. Temperature dependence of oscillation amplitudes for three gate voltages. Sample B. Solid lines are theoretical curves for three effective masses.

Figure 11. Effective masses of the ground state (0), first excited (□), and second excited (Δ) subbands as functions of their respective densities. Solid line is calculation.

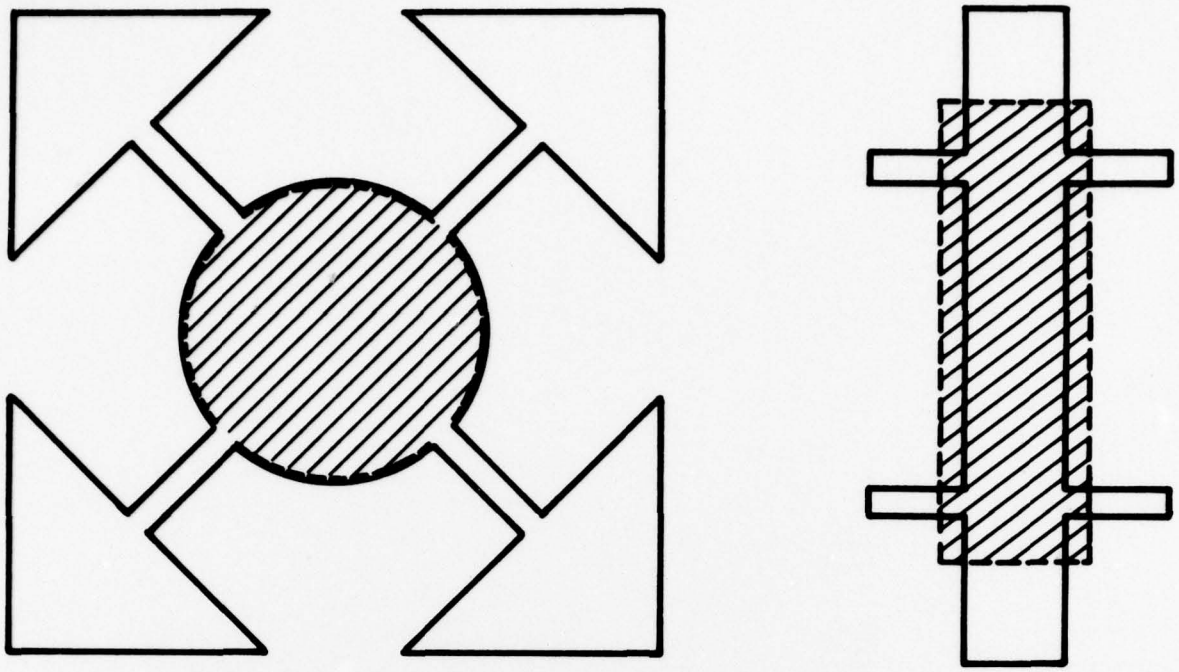

(a)

(b)

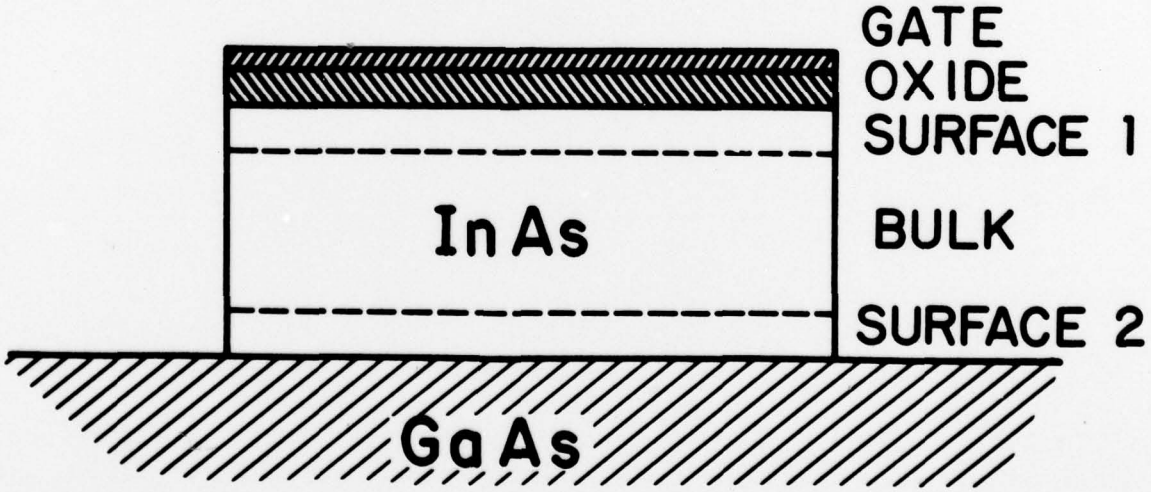

(c)

Figure 1

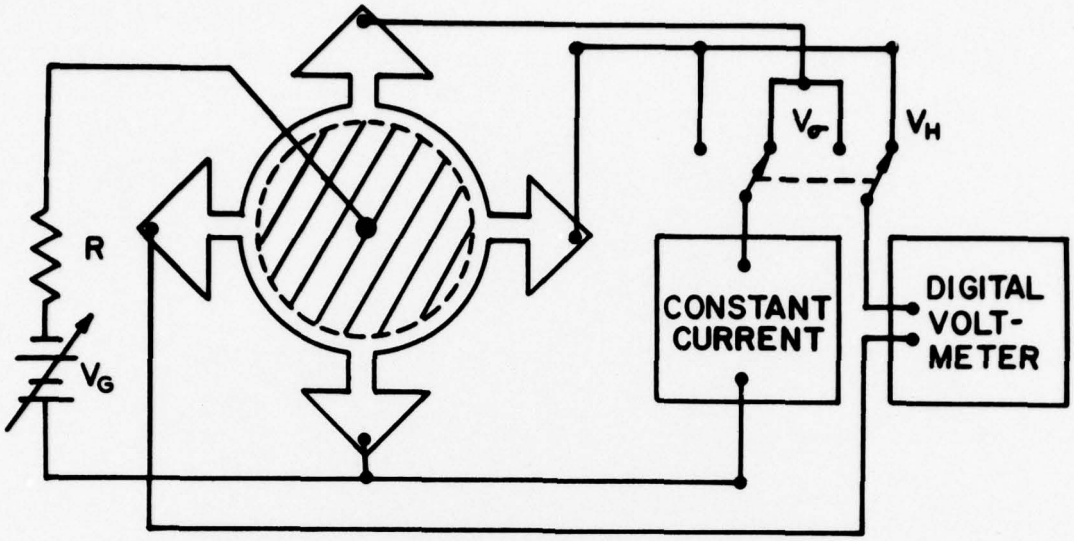
R
V_G
V_σ
V_H
CONSTANT CURRENT
DIGITAL VOLT-METER

(a)

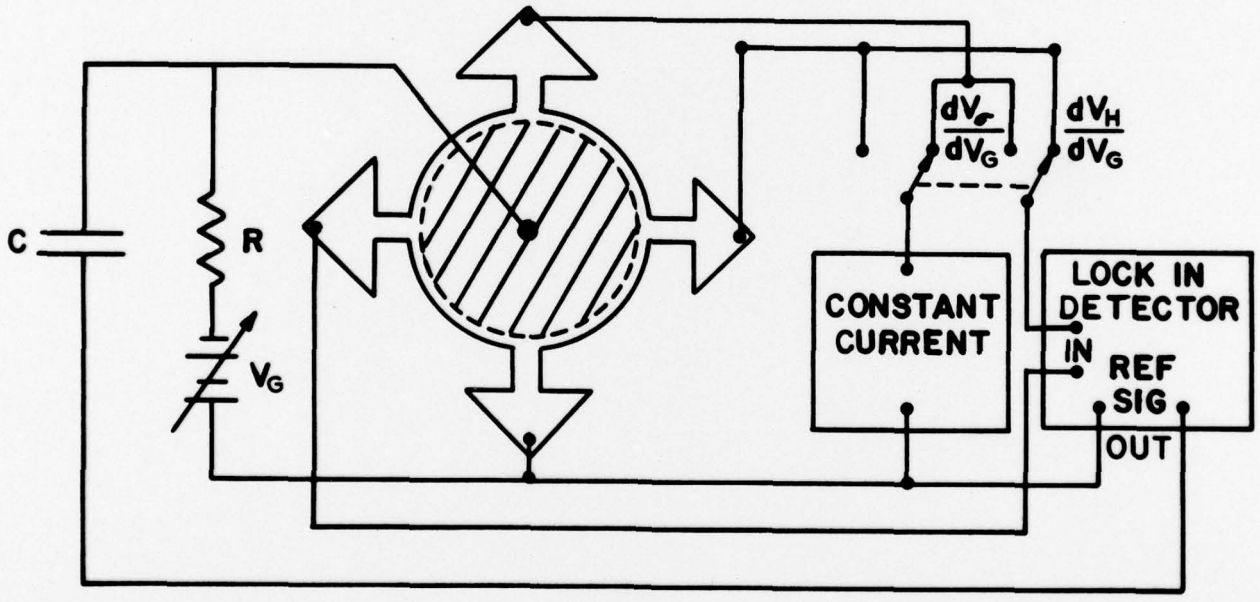
C
R
V_G
$\frac{dV_\sigma}{dV_G}$
$\frac{dV_H}{dV_G}$
CONSTANT CURRENT
LOCK IN DETECTOR
IN
REF
SIG
OUT

(b)

Figure 2

Figure 3

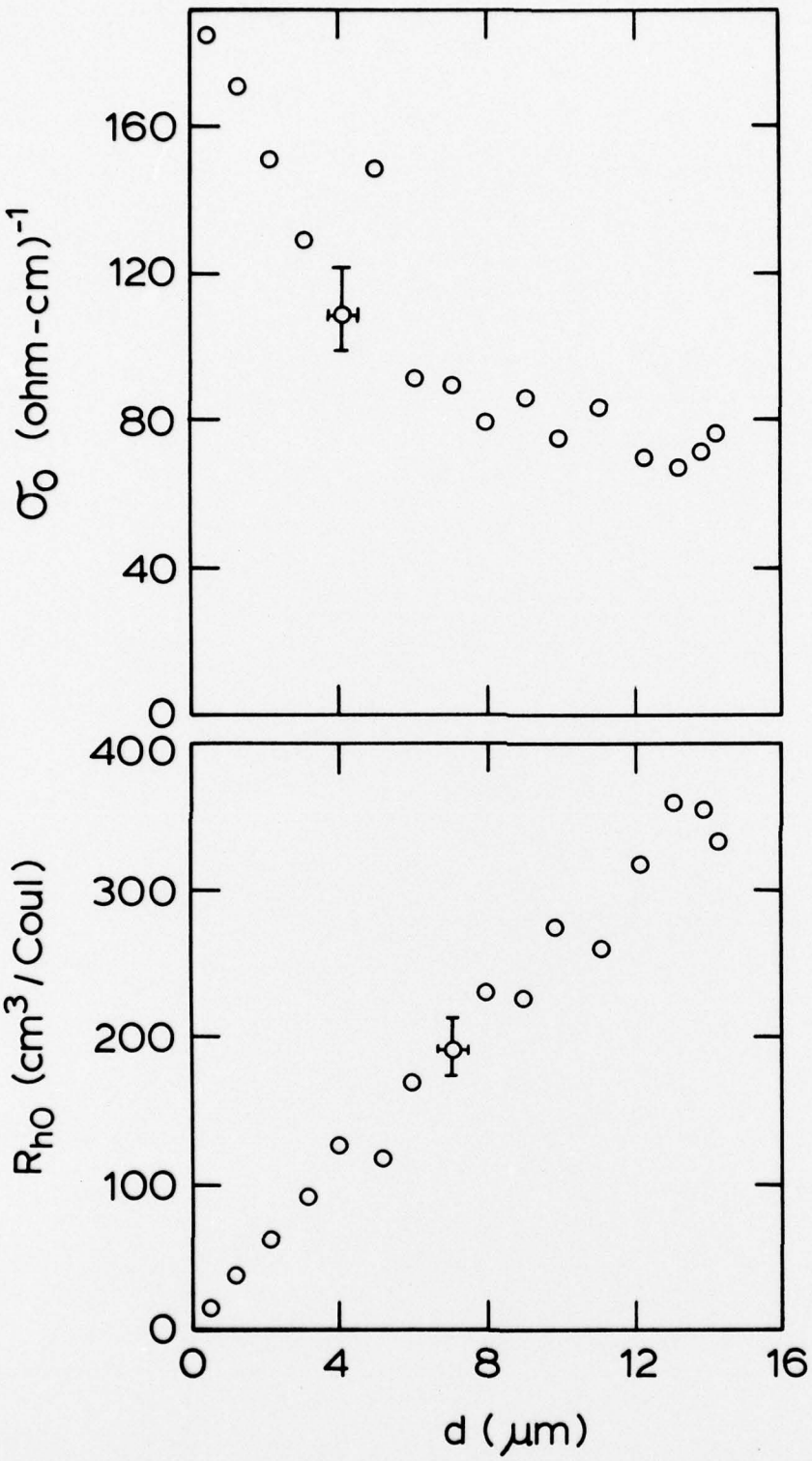
160
120
80
40
0
σ_o (ohm-cm)$^{-1}$
400
300
200
100
0
R_{ho} (cm^3/Coul)
0
4
8
12
16
d (μm)

Figure 4

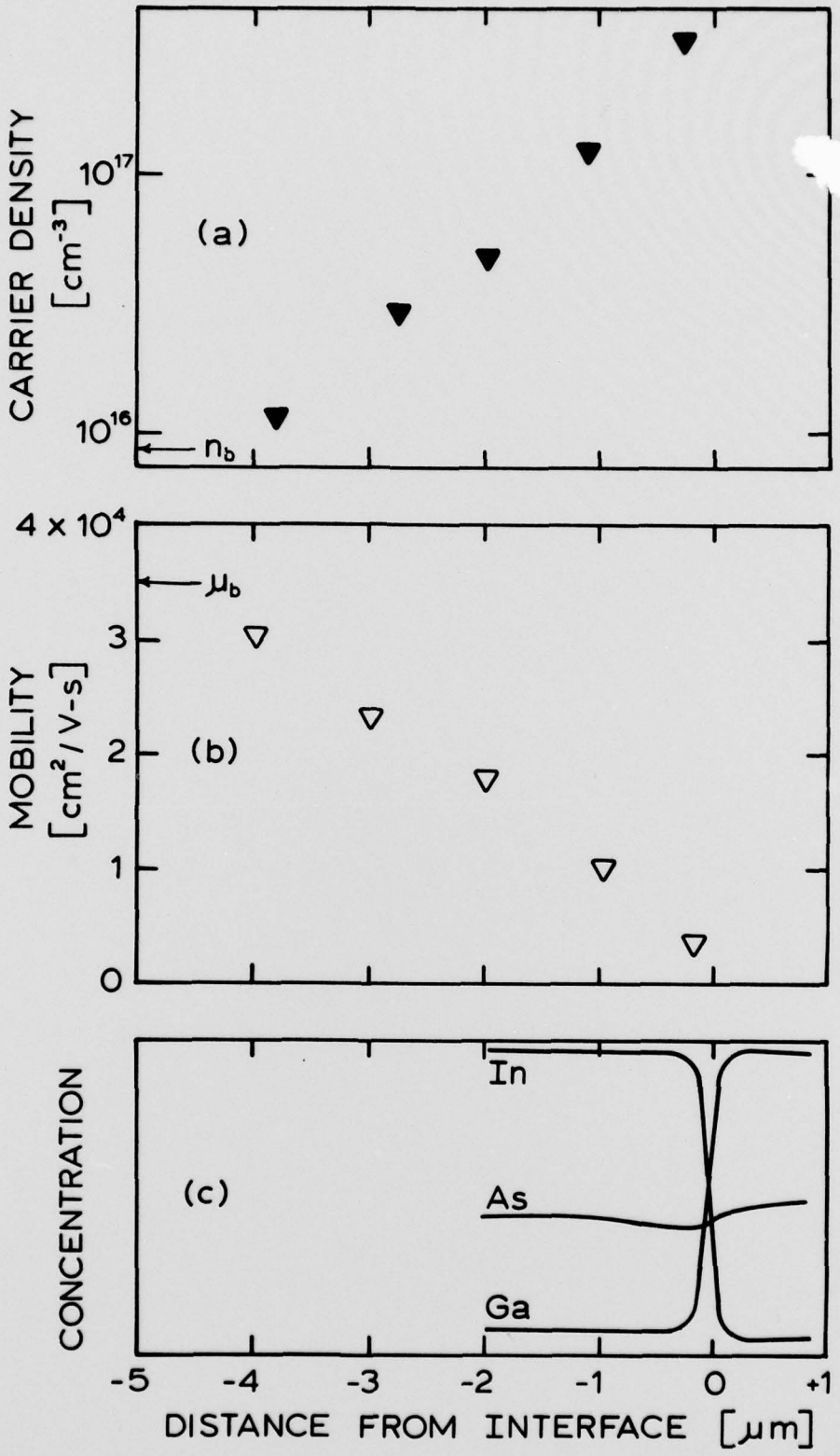
CARRIER DENSITY
[cm⁻³]
10¹⁷
10¹⁶
(a)
n_b
4 x 10⁴
μ_b
3
2
1
0
MOBILITY
[cm²/V-s]
(b)
CONCENTRATION
(c)
In
As
Ga
-5
-4
-3
-2
-1
0
+1
DISTANCE FROM INTERFACE [μm]

Figure 5

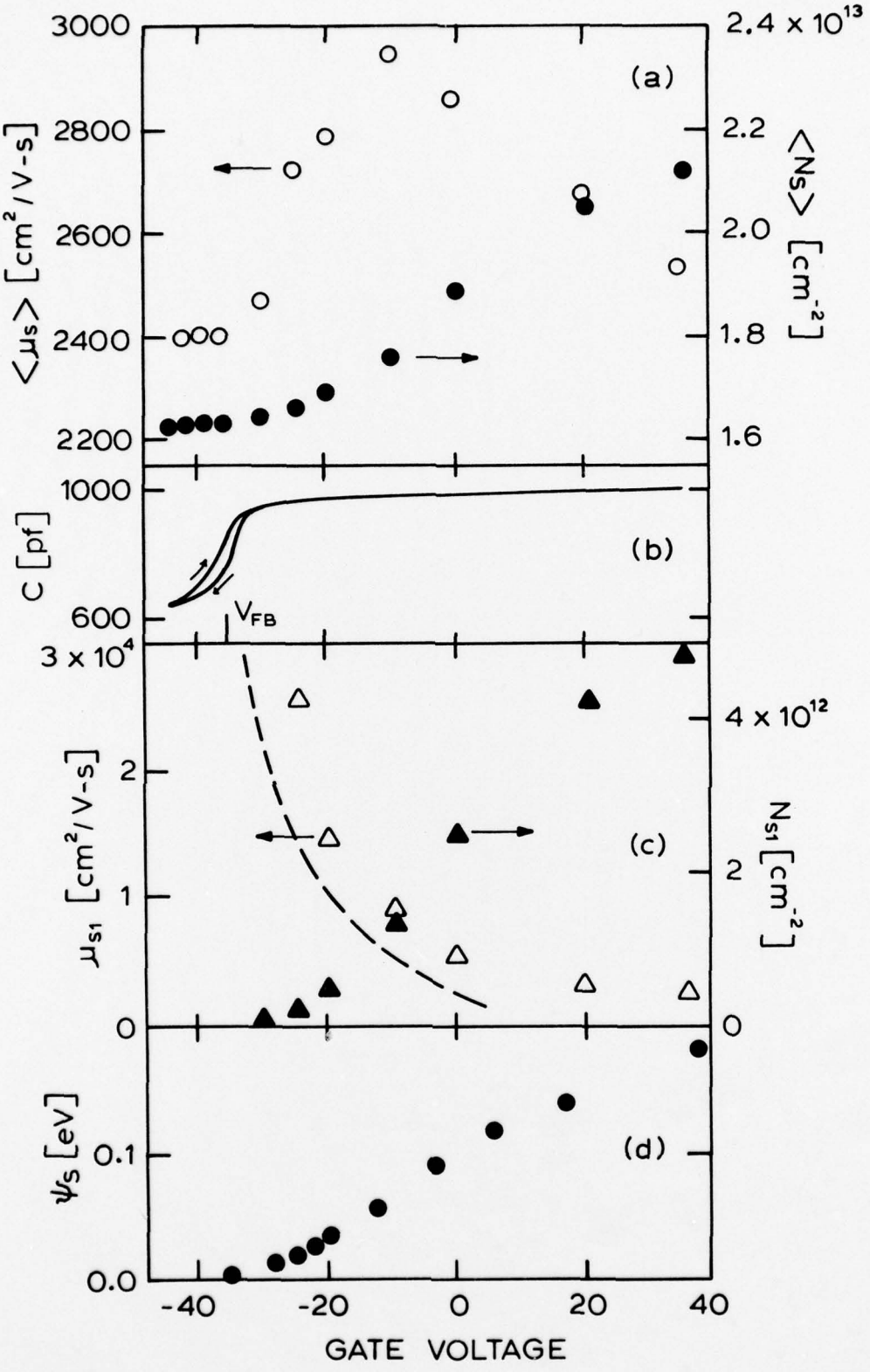
3000
2800
2600
2400
2200
<μs> [cm²/V-s]
2.4 x 10¹³
2.2
2.0
1.8
1.6
<Ns> [cm⁻²]
(a)
1000
600
C [pf]
(b)
V_FB
3 x 10⁴
2
1
0
μs1 [cm²/V-s]
4 x 10¹²
2
0
Ns1 [cm⁻²]
(c)
0.1
0.0
ψs [eV]
(d)
-40
-20
0
20
40
GATE VOLTAGE

Figure 6

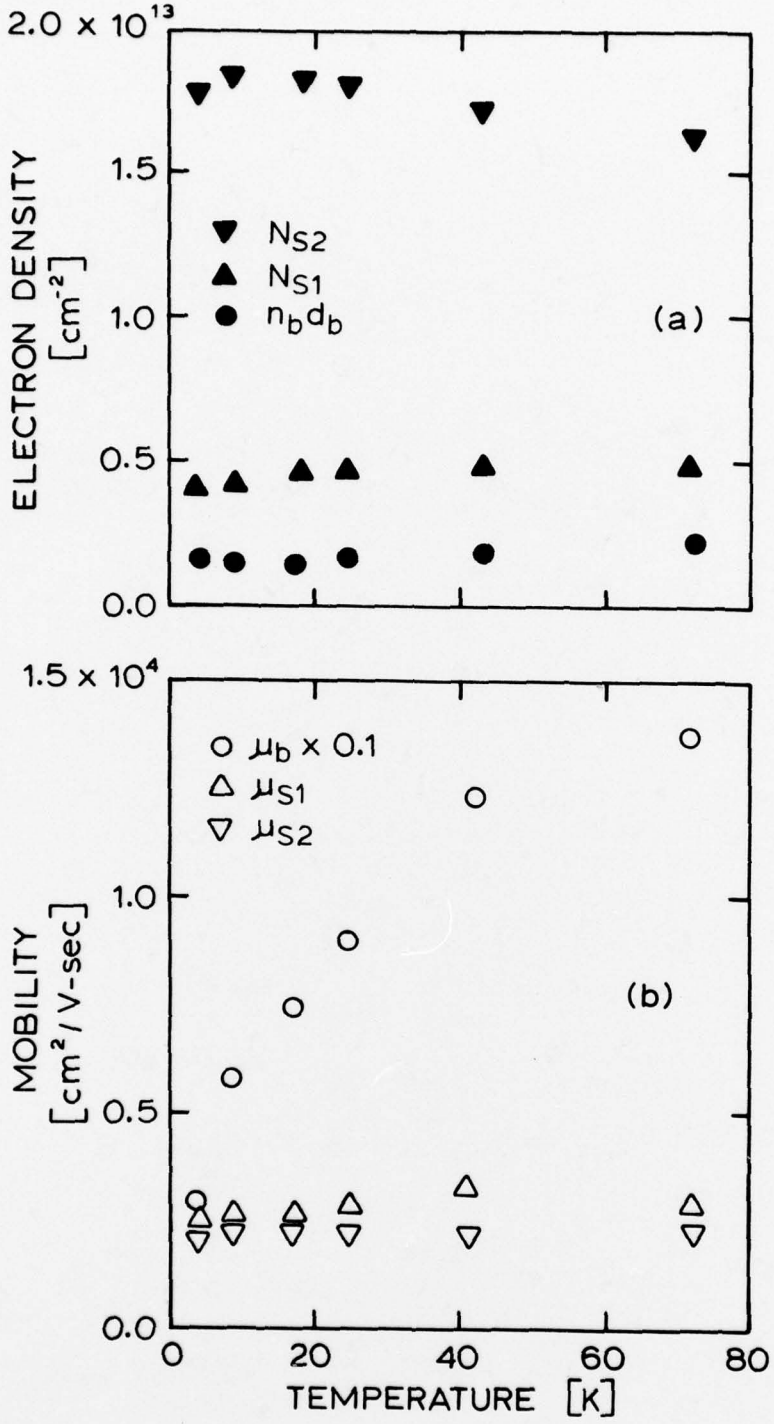
2.0 x 10^13
1.5
1.0
0.5
0.0
ELECTRON DENSITY [cm^-2]
N_S2
N_S1
n_b d_b
(a)
1.5 x 10^4
1.0
0.5
0.0
MOBILITY [cm^2 / V-sec]
μ_b x 0.1
μ_S1
μ_S2
(b)
0
20
40
60
80
TEMPERATURE [K]

Figure 7

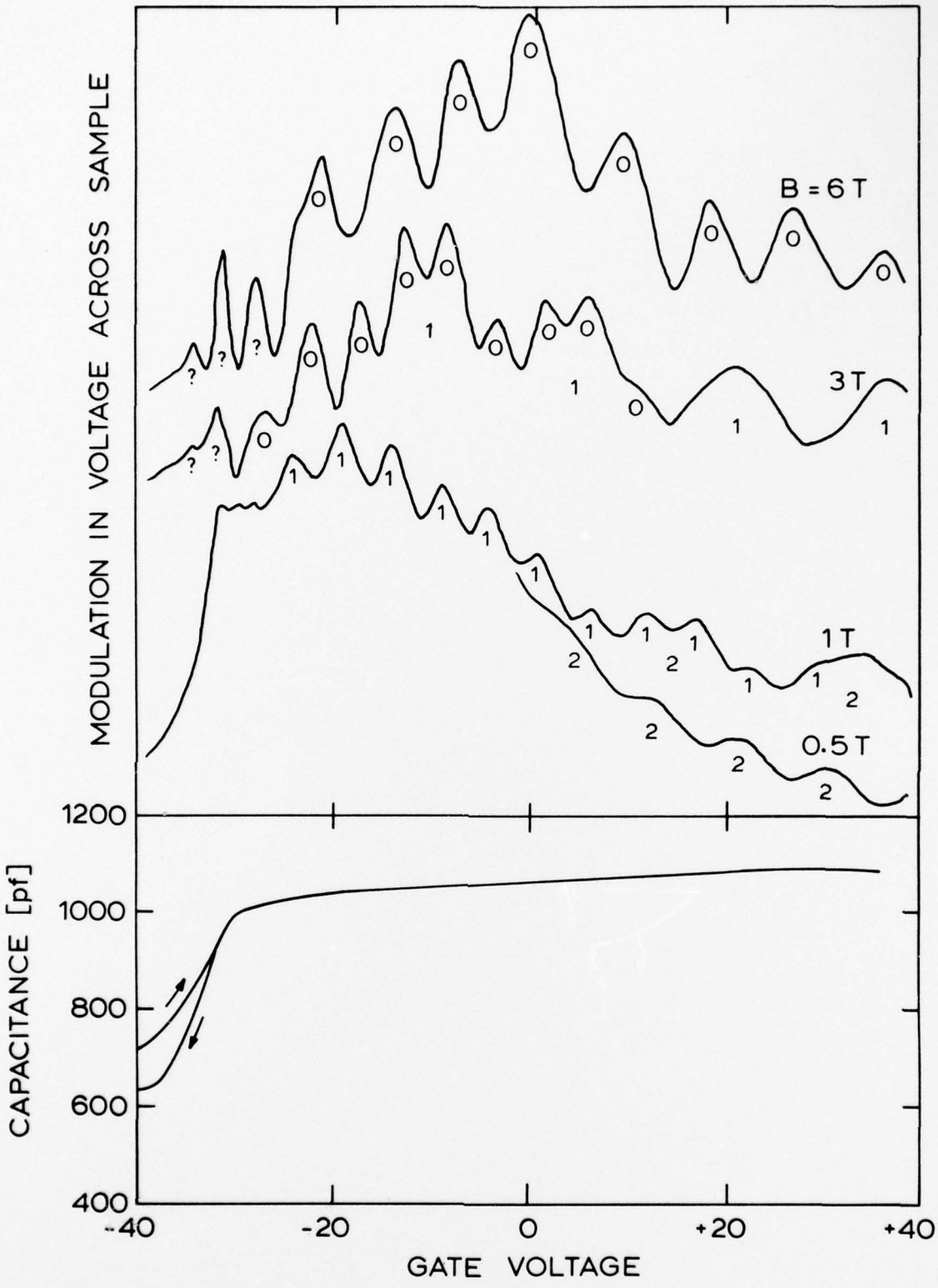
MODULATION IN VOLTAGE ACROSS SAMPLE
B = 6 T
3 T
1 T
0.5 T
CAPACITANCE [pf]
1200
1000
800
600
400
-40
-20
0
+20
+40
GATE VOLTAGE

Figure 8

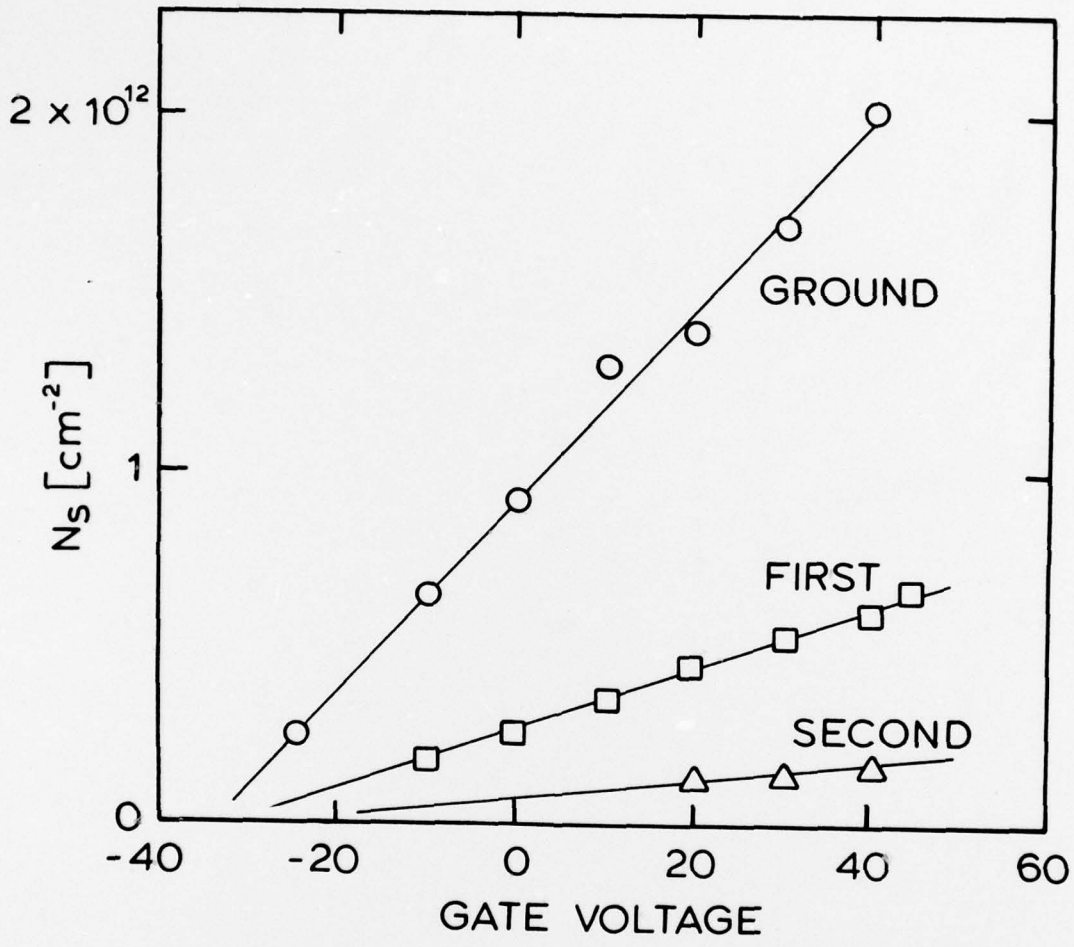
2 x 10^12
1
0
Ns [cm^-2]
GROUND
FIRST
SECOND
-40
-20
0
20
40
60
GATE VOLTAGE

Figure 9

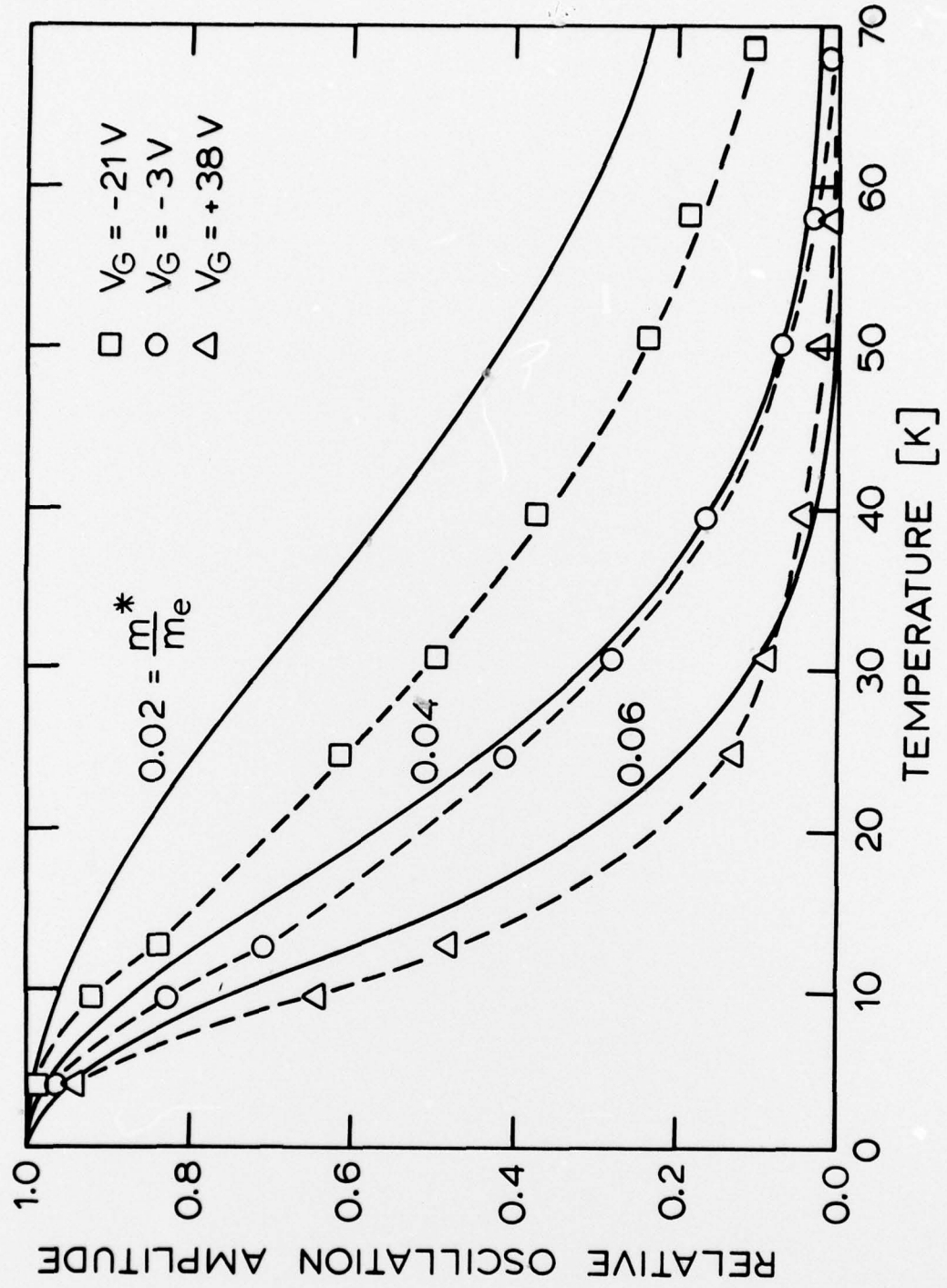
RELATIVE OSCILLATION AMPLITUDE
1.0
0.8
0.6
0.4
0.2
0.0
0
10
20
30
40
50
60
70
TEMPERATURE [K]
V_G = -21 V
V_G = -3 V
V_G = +38 V
0.02 = $\frac{m^*}{m_e}$
0.04
0.06

Figure 10

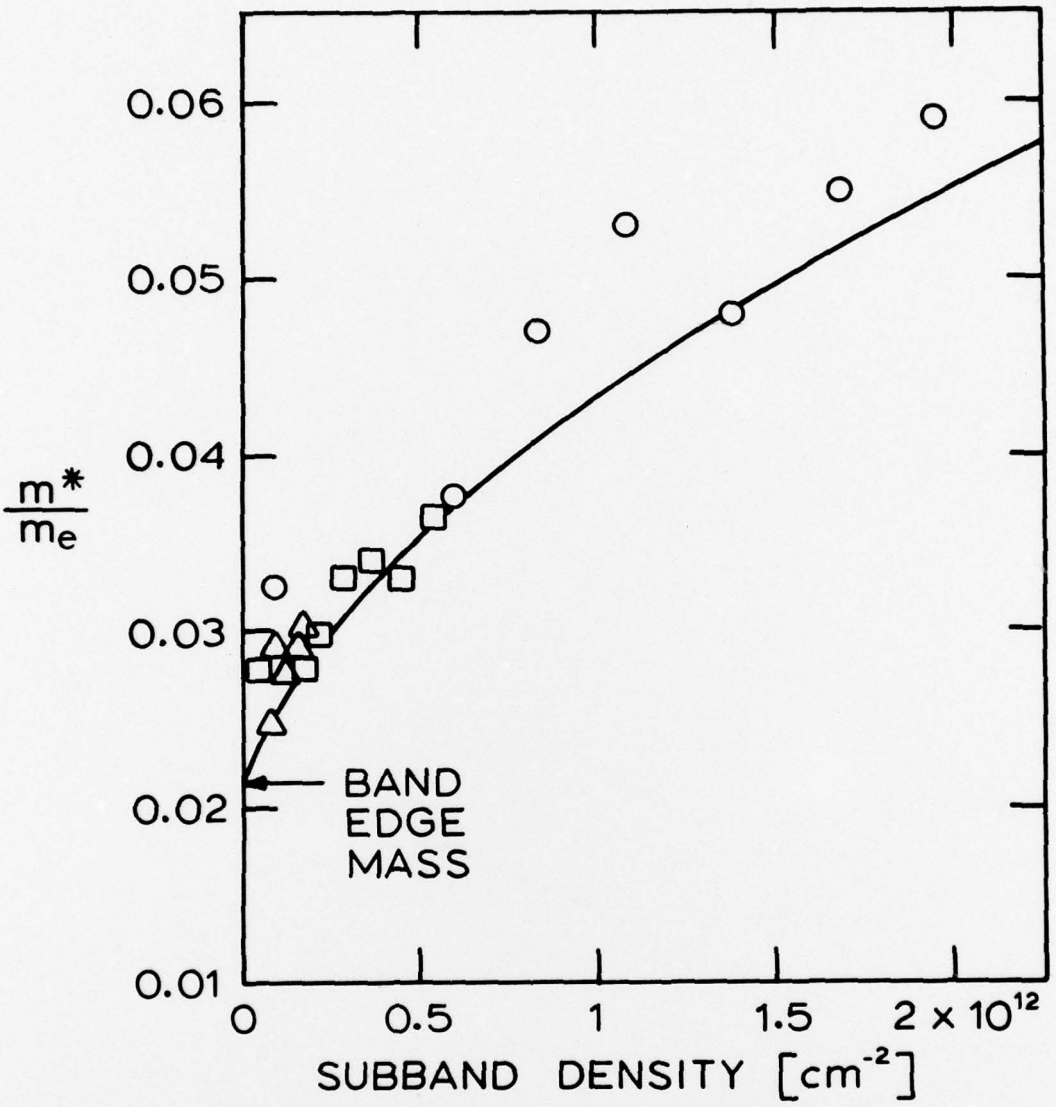
0.06
0.05
0.04
0.03
0.02
0.01
m*/me
BAND
EDGE
MASS
0
0.5
1
1.5
2 x 10^12
SUBBAND DENSITY [cm^-2]

Figure 11

DISTRIBUTION LIST
TR SF 15

Addressee	Number of copies
Office of Naval Research 800 North Quincy Street Code 427 Arlington, Virginia 22217	4
Defense Supply Agency Defense Documentation Center Cameron Station Alexandria, Virginia 22314	12
Naval Research Laboratory 4555 Overlook Avenue, S. W. Washington, D.C. 20375 Attn: H. Dietrich, Code 5212	1
North Carolina State University Department of Electrical Engineering Raleigh, North Carolina 27607 Attn: Dr. M. A. Littlejohn	1
Naval Ocean Systems Center San Diego, California 92152 Attn: Code 0922	1
Stanford University Stanford, California 94305 Attn: Professor Gibbons	1
TRW Defense and Space Systems Group One Space Park Redondo Beach, California 90278 Attn: T. Mills	1
Texas Instruments, Inc. P. O. Box 5936 *Dallas, Texas* 75222 Attn: Don Shaw	1
Raytheon Company Waltham, Massachusetts 02154 Attn: R. Berig	1
Varian Associates Palo Alto, California 94303 Attn: R. Bell	1

Addressee	Number of copies
Westinghouse Research Laboratory 1310 Beulah Road Pittsburgh, PA 15235 Attn: H. C. Nathanson	1
RCA Laboratories David Sarnoff Research Center Princeton, New Jersey 08540 Attn: Y. Narayan	1
Advisory Group on Electron Devices 201 Varick Street 9th floor New York, New York 10014	1
Dr. Y. S. Park AFAL/DHR Building 450 WPAFB, Ohio 45433	1
Dr. R. Eden Rockwell Science Center P. O. Box 1085 Thousand Oaks, CA 91360	1